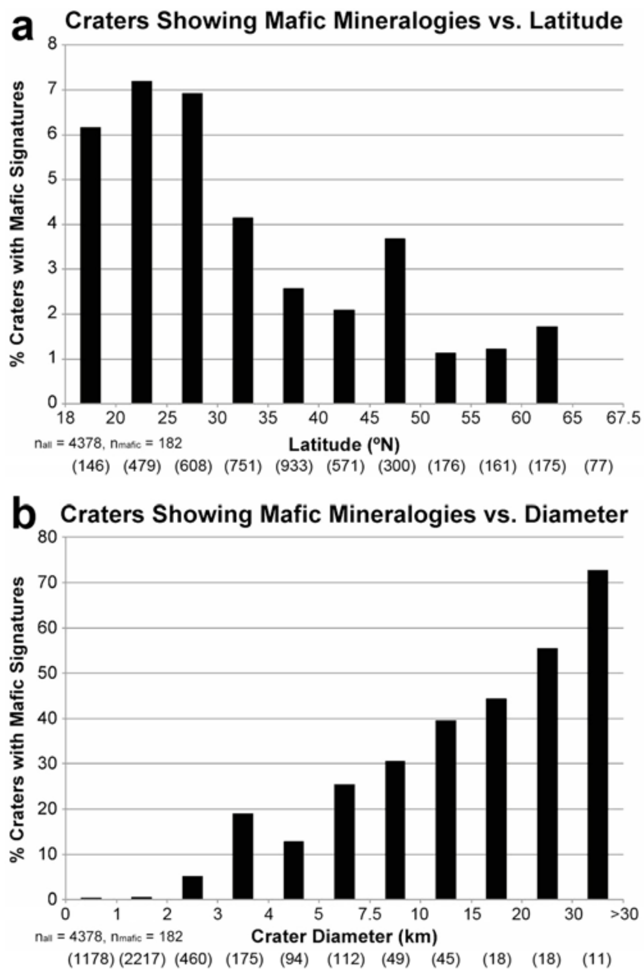

Figure 5. (a) The percentage of craters showing mafic signatures versus latitude. (b) The percentage of craters showing mafic signatures versus crater diameter. The numbers in parentheses represent the total number of craters in each bin.

[17] In total, 4377 craters were observed with CRISM data throughout the study region; 126 were identified in CRISM targeted images, while the remaining craters were identified with CRISM mapping tiles with some targeted image overlap. These craters range in diameter from 0.3 to 67.1 km. Of the 4377 craters, 182 craters in Acidalia and Chryse planitiae were found to have mafic signatures associated with in situ bedrock material (i.e., not associated with mobile dunes or other wind-blown accumulations), 38 of which were identified using CRISM targeted imagery. Figure 4 shows the location of all craters observed in both the CRISM multispectral mapping tiles and targeted observations in Acidalia and Chryse planitiae (black dots) and those which were found to exhibit mafic signatures (white dots). The mafic signatures associated with these craters were first identified using the OLINDEX2 and HCPINDEX spectral parameters and then verified by detailed spectral analyses. The availability of targeted CRISM images is likely the limiting factor in the identification of mafic mineralogies. The additional acquisition of targeted images of impact craters throughout the region will likely reveal the presence of many more craters that show underlying mafic compositions.

[18] The percentage of craters that reveal mafic signatures shows an apparent relationship with latitude. At latitudes lower than 30°N, 6%–8% of craters show mafic signatures. The percentage of craters showing mafic signatures steadily decreases with increasing latitude to less than 2% at latitudes greater than 50°N (Figure 5a). Additionally, there is a strong relationship between crater size and the percentage of craters with observed mafic mineralogies (Figure 5b). The lesser number of small craters that show mafic signatures, however, may be the result of the inability for CRISM to detect thin layers of mafic material along the walls of small craters using the lower-resolution mapping tiles. This sampling bias may be resolved by acquiring high-resolution CRISM images of craters observed in mapping tiles to verify that they lack mafic signatures.

[19] HiRISE and CTX data were used to better constrain the relationship between the presence of mafic signatures and crater size and latitude. The presence of olivine and clinopyroxene appears to be associated with distinct bedrock layers that are well defined in southern Acidalia and Chryse planitiae and less defined and better obscured in northern Acidalia Planitia. In Chryse Planitia and southern Acidalia Planitia, mafic signatures are found in exposed near-surface layers within crater walls. Using HiRISE and CTX data in conjunction with CRISM reveals that these mafic layers are present within several meters to tens of meters of the undisturbed surface. Further north into central and northern Acidalia Planitia, the mafic signatures become absent from near-surface layers in crater walls and are restricted primarily to crater ejecta and central peaks. Additionally, there is a strong preference in observed mafic signatures along equator-facing slopes, while these signatures are generally absent or extremely subdued along pole-facing slopes.

3.1. Representative Observations

[20] In this section, craters exhibiting mafic signatures are analyzed and their relevance and context within the study region are discussed. The examples are arranged in order of increasing latitude to highlight the latitudinal variations observed throughout the study region. They are also representative of craters at their particular latitude and capture in detail the geologic relationships between the observed composition and stratigraphy.

[21] CRISM image FRT00009A9A of Naar Crater in Chryse Planitia (22.87°N, 317.80°E) is shown in Figure 6 and is a prime example of low-latitude craters in the study region. The image on the left is an OLINDEX2 parameter map where brighter shades of gray indicate a stronger 1 μm olivine absorption feature and darker shades of gray indicate a weaker 1 μm feature. OLINDEX2 shows distinct enrichments in olivine along the northeastern wall of the crater (Figure 6). This enrichment was then verified using detailed spectroscopic analyses to ensure that olivine was the mineral being detected (Figure 6). A more detailed look at this region reveals a distinct sequence of mafic mineralogies at different stratigraphic horizons within the crater wall and central peak, as shown in Figure 7. Material exposed in the crater wall (units 1–4) and central peak (unit 5) alternate between olivine- and clinopyroxene-bearing; units 1 and 3 are dominated by olivine, while units 2 and 5 are dominated by clinopyroxene. Unit 4 consists primarily of talus material derived from the crater wall (as shown in HiRISE data) and